forests

Article

Carnivorous Plant Algorithm and BP to Predict Optimum Bonding Strength of Heat-Treated Woods

Yue Wang, Wei Wang * and Yao Chen

College of Engineering and Technology, Northeast Forestry University, Harbin 150040, China
* Correspondence: vickywong@nefu.edu.cn; Tel.: +86-133-1361-3588

Abstract: In this study, the CPA algorithm was used to optimize a BP neural network model to predict the bond strength and surface roughness of heat-treated wood. The neural network model was trained and optimized using MATLAB software. The results of the BP neural network, random forest algorithm, and optimized CPA-BP model were compared. The results show that the CPA-optimized BP neural network model has a better R^2 compared to the conventional BP neural network model. After using the CPA-optimized BP neural network model, the R^2 value increased by 8.1%, the MAPE value decreased by 3.74%, and the MAE value decreased by 33.91% in the prediction of the surface bond strength. The R^2 values increased by 3.02% and 20.47%, respectively, in predicting the mean and maximum values of surface roughness. The results indicate that the model is reliable in predicting wood bond strength and wood surface roughness. Using this model to predict wood bond strength and surface roughness can also reduce the required experimental cost.

Keywords: carnivorous plant algorithm; BP neural network model; random forests; wood heat treatment

1. Introduction

Compared with untreated wood, heat-treated wood has better dimensional stability and durability and can improve wood appearance defects such as blue stain [1]. Using heat-treated wood to produce plywood is one of the most important ways to improve the durability of plywood. After the high-temperature heat treatment of solid wood-sawn timber, the control of its bonding properties is very important to improve the quality of plywood. However, as wood is an anisotropic material, during the wood gluing process, if the configuration of the fiber direction on the wood gluing surface is changed, its gluing strength will change. Moreover, different wood species, densities, materials, properties, and types of wood-based panels have different bonding strengths. For example, ash and beech have better bearing capacities, but it is difficult for these tree species to obtain higher bonding durability [2,3]. Therefore, the bonding quality test is affected by many variables, such as primer type, tree species, dry sandpaper particle size, wood grain direction, etc. This results in a significant amount of time and cost when assessing the bonding properties of wood surfaces. Therefore, establishing a reliable test procedure to effectively evaluate the gluing quality is still a matter of great concern [4].

The first reports of the thermal modification of wood date back to 1915, when Harry Tiemann heated air-dried wood in superheated steam at 150 °C and found a reduction in the hygroscopicity of TMT [5].

The authors selected European oak as the subject of their experiments, and all samples were subjected to air conditioning under specific conditions (65% ± 3% relative humidity and 20 ± 2 °C) for more than 6 months to achieve an equilibrium moisture content (EMC) of 12%. It was concluded that these structural changes in the main components of the wood have a significant impact on the various properties of thermally modified wood [6].

The experimental results show that thermal modification of Pinus oocarpa wood at 17 °C, as required by Colombian standards, leads to higher density and resistance and improved dimensional stability, favoring their application for structural purposes [7].

check for updates

Citation: Wang, Y.; Wang, W.; Chen, Y. Carnivorous Plant Algorithm and BP to Predict Optimum Bonding Strength of Heat-Treated Woods. *Forests* **2023**, *14*, 51. https://doi.org/10.3390/f14010051

Academic Editors: Tomasz Krystofiak and Pavlo Bekhta

Received: 21 November 2022
Revised: 13 December 2022
Accepted: 13 December 2022
Published: 27 December 2022

Altgen et al. (2016b) [8] presented a similar trend for European beech, as the CML increased with higher pressure and the same temperature. Even at lower temperatures and shorter total processing times, modification in a closed system under high pressure had a greater effect on the chemical structure of the modified wood than modification in an open system [8].

The wood was thermally modified (TM) at 150, 170, and 190 °C for 2, 4, and 6 h, respectively [9].

Many scholars have carried out related research. Machine learning algorithms have gained widespread popularity because they are low-cost, efficient, and do not require any prior knowledge [10].

Erik Serrano [11] investigated the susceptibility of various wood-binder adhesion test methods for geometric defects using nonlinear finite element analysis.

Luis Garcia Esteban et al. [12] developed an artificial neural network as a prediction method with the aim of determining the suitability of board bonding in less time. In the end, a prediction accuracy of 93% was achieved.

Cenk Demirkir et al. [13] took the wood type, density, veneer peeling temperature, veneer drying temperature, and adhesive type as considerations, and designed an artificial neural network that could predict the optimal manufacturing parameters of plywood.

Bruna Ugulino et al. [14] applied ANOVA to evaluate surface quality by roughness, scanning electron micrographs, and wettability analysis. They concluded that using a rake angle of 25° and a short or medium wavelength should be suitable for perimeter planing on red oak surfaces.

Ender Hazir et al. [15] proposed a hybrid SVR-GA and ELM-GA method to predict the bond strength of wood coatings with temperature, time, cutting speed, feed rate, and particle size as process factors.

However, at present, the influence of surface roughness on the bonding performance of plywood is less involved in the research on the prediction of the bonding performance of plywood, and the selection of tree species is relatively simple. The roughness of the glued surface directly affects the formation of the glue layer and the glue strength. Therefore, in order to better study the effect of different tree species and roughness on the bonding performance, four tree species were selected in this paper, namely, *Pinus sylvestris* L., Oriental beech (*Fagus orientalis* L.), white oak (*Quercus petraea* spp.), and Uludag fir (*Abies Bornmulleriana* mattf.). Finally, the carnivorous plant algorithm (CPA) was used to optimize the weights and thresholds of the BP network to predict its bonding properties and surface roughness, respectively, in order to achieve a more accurate prediction effect.

In summary, this paper uses the CPA-BP algorithm to predict the bond strength and surface roughness of heat-treated wood, aiming to provide a basis for the determination of the bond quality of composite boards.

2. Methods

Bond strength is a very important reference parameter when measuring the properties of wood itself. Heat treatment, wood type, feed rate, adhesive type, etc. all have an effect on its bond strength.

2.1. Data Preparation

The data used in this study were derived from previous experimental studies by Ozcan. In Ozcan's study, experiments were conducted on four kinds of wood, Scotch pine, eastern beech, white oak, and Uludag fir, to determine the effect of heat treatment on their bond strength [16].

All samples in this experiment were conditioned in a climate chamber controlled at a temperature between 20 ± 2 °C and a humidity of 65% ± 5% until an average moisture content of 12% was reached. The samples were cut in radial and tangential directions using feed speeds of 8 and 16 m/min. Using polyvinyl acetate (PVAc) and melamine-urea-formaldehyde (MUF) as binders, the samples were coated at a rate of 200 g/m^2. At

100 °C, the density of PVAc is 1.1 g/m^2 and that of MUF is 1.22 g/m^2. The samples were compressed with a pressure of 2 kgf/cm^2 for 6 h PVAc and 5 min MUF and then tested on the testing machine. The samples were then placed in laboratory ovens at temperatures of 120 °C, 150 °C, and 180 °C for 2 h and 6 h for heat treatment. After each heat treatment, the samples need to continue to be conditioned in the climate chamber until an average moisture content of 10% is reached, and then the bond strength of the samples is calculated.

In this study, the bond strength was predicted by the carnivorous plant algorithm and the BP neural network. Use MATLAB to train and optimize the model. The experimental data are divided into training sets and test sets, of which 54 sets are used for the training process and 10 sets are used for the testing process.

T-Test and ANOVA

A *t*-test is used to compare whether there is a significant difference between the means of the two samples. The independent samples *t*-test (unpaired two samples test) used in this paper is used to compare two independent sample means. ANOVA is mainly used to test the significance of the difference between the means of two and more samples. The data obtained from the study show fluctuations due to various factors. The causes of fluctuations can be divided into two categories: uncontrollable random factors and controllable factors imposed in the study that form an impact on the results. Both sets of data used in this paper contain four sets of independent variables, and in order to analyze the magnitude of the effect of changes in different variables on the surface bond strength and surface roughness of the last four tree species, independent sample tests, and one-way ANOVA analysis were performed using SPSS software (Version 27, 2020, IBM Corp, Armonk, NY, USA).

Among them, a *t*-test was used for the variables of feeding speed and time, duration, and adhesives, while the temperature and heat treatment were controlled using an ANOVA test. All data analyses were performed at 95% confidence intervals. The multiple comparison method of LSD was utilized, which is the most widely used of all comparison methods, has a higher test efficacy, and is more sensitive to differences.

Tables 1 and 2 show the results of the *t*-test between adhesives and scotch pine. Because the independent variable under discussion at this point is the type of binder and there are only two types, the *t*-test is chosen here. The first table shows that there is some variability in the mean value of 6.3531 when the binder is MUF and 10.6188 when the binder is PVAc. The significance in Table 2 is 0.002, which is less than 0.05, indicating the existence of significant differences.

Table 1. Scotch pine's *t*-test analysis for adhesives. (Group Statistics).

Group Statistics					
Adhesives		N	average value	Standard deviation	Standard error mean
ScotchPine	0.00	32	6.3531	0.79189	0.13999
	1.00	32	10.6188	1.56750	0.27710

Table 2. Scotch pine's *t*-test analysis for adhesives. (Independent sample test).

Independent Sample Test									
	Levin's test of variance equality		Mean equality t-test						
ScotchPine	F	Significance	t	degree of freedom	Significance (two-tailed)	Mean Difference	Standard error difference	Difference 95% confidence interval	
								Lower limit	Upper limit
Assuming equal variance	10.641	0.002	−13.740	62	0.000	−4.26563	0.31045	−4.88621	−3.64504
Does not assume equal variance			−13.740	45.856	0.000	−4.26563	0.31045	−4.89058	−3.64067

Tables 3 and 4 show the ANOVA test with time as the independent variable and the surface bond strength of scotch pine as the dependent variable. In Table 3, the significant difference of 0.013 is less than 0.05, indicating that there is a significant difference, and in the post hoc test, the LSD test was taken for further analysis. In Table 4, it can be clearly seen that the significant differences were greater at 150 and 180 degrees Celsius without heat treatment; at 120 degrees Celsius and at 180 degrees Celsius, the results of the surface bond strength were greater.

Table 3. ANOVA of scotch pine for temperature.

Scotch Pine	Sum of Squares	Degree of Freedom	Mean Square	F	Significance
SSA	62.747	3	20.916	3.873	0.013
SSE	323.991	60	5.400		
SST	386.737	63			

Table 4. Multiple comparisons (LSD).

(I) Temp	(J) Temp	Mean Difference (I–J)	Standard Error	Significance	95% Confidence Interval	
					Lower Limit	Upper Limit
0.00	1.00	1.00625	0.82157	0.225	−0.6371	2.6496
	2.00	1.86250 *	0.82157	0.027	0.2191	3.5059
	3.00	2.66250 *	0.82157	0.002	1.0191	4.3059
1.00	0.00	−1.00625	0.82157	0.225	−2.6496	0.6371
	2.00	0.85625	0.82157	0.301	−0.7871	2.4996
	3.00	1.65625 *	0.82157	0.048	0.0129	3.2996
2.00	0.00	−1.86250 *	0.82157	0.027	−3.5059	−0.2191
	1.00	−0.85625	0.82157	0.301	−2.4996	0.7871
	3.00	0.80000	0.82157	0.334	−0.8434	2.4434
3.00	0.00	−2.66250 *	0.82157	0.002	−4.3059	−1.0191
	1.00	−1.65625 *	0.82157	0.048	−3.2996	−0.0129
	2.00	−0.80000	0.82157	0.334	−2.4434	0.8434

* The significance level of the mean difference was 0.05.

The variables with significant differences for the other corresponding tree species can be obtained in the same way using SPSS. In the analysis of the surface bond strength data, the following results were obtained: feeding speed and duration did not have a significant effect on the output results, while the binder type and temperature were significant differences in the outcome variables for all four species. The effect of temperature was a bit greater compared to the binder type and temperature. In the analysis of the surface roughness, the following results were obtained: there was a significant difference in the outcome variable of surface roughness between feeding speed, heat treatment temperature, and whether heat treatment was performed or not, while there was no significant difference in the change of time. When discussing the surface roughness and the mean and maximum values, the effect on the maximum value before and after heat treatment was higher than the mean value.

2.2. Prediction Models

2.2.1. Carnivorous Plant Algorithm (CPA)

Biomimetic and population-based metaheuristic algorithms such as the ant colony algorithm and the sparrow algorithm are widely used today. The metaheuristic algorithm is an improvement of the heuristic algorithm, which is a combination of the randomized algorithm and the local search algorithm [17]. CPA is also a meta-heuristic algorithm, which can successfully solve problems such as high-dimensional design variables, the existence of various constraints, and the search space with many local optimal solutions. It can search globally, avoid falling into local optimum, and obtain high-precision solutions from ideal regions, which can prevent premature convergence in the process of optimization. It mimics how carnivorous plants adapt and improve their survivability in harsh environments.

CPA starts by randomly initializing a set of solutions that are divided into carnivorous plants and prey, grouped according to their growth and reproduction processes. Then, update the fitness value and combine all solutions. This process needs to be repeated until the termination condition is met.

The first is initialization, which needs to be randomly initialized in the wetland among *n* individuals consisting of carnivorous plants and prey. The number of carnivorous plants and prey is represented in the form of a matrix by n*CPlant* and n*Prey*, respectively. Each individual is randomly initialized using the following method:

$$Individual_{i,j} = Lb_j + \left(Ub_j - Lb_j\right) \times rand \tag{1}$$

where *Lb* and *Ub* are the lower bound and upper bound of the search domain, respectively, with $i = 1, 2, \ldots, n$ and $j = 1, 2, \ldots$, d. Rand is a random number drawn from the range [0, 1].

Replace each individual with a predefined fitness function to evaluate its fitness. For the minimization case, the lower the number of fitness values, the higher the quality of the solution vector.

The next step is to sort them in ascending order based on their fitness values. The highest n*CPlant* solution in the population was selected as the carnivorous plant, while the other solutions were regarded as the prey n*Prey*. During the grouping process, the prey with the highest fitness is assigned to the first-ranked carnivorous plant, and the second and third-ranked preys are similarly assigned to the second and third carnivorous plants. The possibility of plant growth is crucial.

Due to various uncertainties, prey may intermittently escape the control of carnivorous plants, so an attraction rate needs to be introduced. For each group of plants, a prey will be randomly selected. If the attraction rate is higher than a randomly generated number, the prey will be captured and digested by carnivorous plants to promote growth. This new carnivorous plant growth model is as follows:

$$NewCP_{i,j} = growth \times CP_{i,j} + (1 - growth) \times Prey_{v,j} \tag{2}$$

$$growth = growth\_rate \times rand_{i,j} \tag{3}$$

where $CP_{i,j}$, is the *i*th ranked carnivorous plant, $Prey_{v,j}$, is the randomly chosen prey, the growth rate is the predefined value, and rand is the random value chosen from the range [0, 1]. In CPA, there is only one carnivorous plant in each group, while the number of preys must be more than two. The attraction rate in CPA is assigned as 0.8 for most cases.

In CPA, there is only one carnivorous plant in each group, but there must be more than two species of prey. In most cases, the CPA has an attraction rate of 0.8; if the attraction rate is lower than the random value generated and the prey escapes the trap and continues to grow, the model is as follows:

$$NewPrey_{i,j} = growth \times Prey_{u,j} + (1 - growth) \times Prey_{v,j}, u \neq v \tag{4}$$

$$growth = growth\_rate \times rand_{i,j},\ f(prey_v) > f(prey_u) \tag{5}$$

$$growth = 1 - growth\_rate \times rand_{i,j}, f(prey_v) < f(prey_u) \tag{6}$$

where $Prey_{u,j}$, is another randomly selected prey in the *i*th ranked group. At this point, an appropriate growth rate needs to be selected.

Carnivorous plants reproduce only for the number one carnivorous plant, that is, the best solution in the population, which can avoid the use of other unnecessary schemes and save the calculation cost:

$$NewCP_{i,j} = CP_{i,j} + Reproduction\_rate \times rand_{i,j} \times mate_{i,j} \tag{7}$$

$$mate_{i,j} = CP_{v,j} - CP_{i,j},\ f(CP_i) > f(CP_v) \quad (8)$$

$$mate_{i,j} = CP_{i,j} - CP_{v,j},\ f(CP_i) < f(CP_v) \quad (9)$$

Among them, where $CP_{i,j}$ is the best solution, $CP_{v,j}$ is the randomly selected carnivorous plant, and the reproduction rate is a predefined value for exploitation.

Finally, the newly produced carnivorous plants and prey combine with the previous population to form a new group. The process of sorting, grouping, growing, and breeding is repeated until the stopping condition is met.

2.2.2. BP Neural Network

BP (Back Propagation) neural network, that is, the learning process of the error back-propagation algorithm is composed of two processes: forward propagation of information and backpropagation of errors. From the input layer to the hidden layer, and then from the hidden layer to the output layer, after comparing with the actual experimental data, when the actual output does not match the expected output, it enters the back-propagation stage of the error. The error is passed through the output layer, and the weights of each layer are corrected according to the method of error gradient descent, and the hidden layer and the input layer are backpropagated layer by layer [18]. The original data information is continuously propagated forward, and the error value is propagated back. This process is the process of continuously adjusting the weights of each layer, which is also the process of learning and training the BP neural network. The disadvantage of the BP neural network is that it is easy to form a local minimum value and cannot obtain a global optimal value. Too many training times also lowers the learning efficiency and slows the convergence speed [19].

In this paper, BP neural network model is used to predict the bond strength and surface roughness of four different tree species, and two prediction models are established, respectively with temperature, adhesive type, tree species, and feeding time as input nodes. Its model performance is shown in Figure 1:

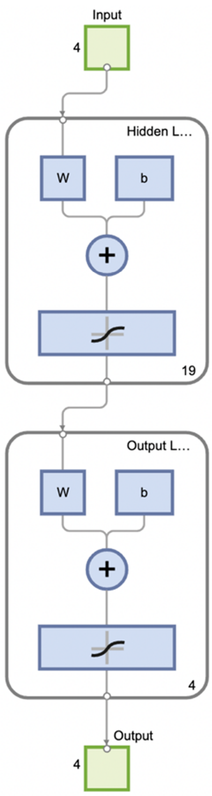

Figure 1. Determination of the node number of the input layer and the output layer.

The data were divided into training and test sets by 64 sets and brought into MATLAB 2021 for manipulation. The BP neural network algorithm was used to predict the bond strength of wood after heat treatment.

2.2.3. Random Forests Algorithm (RF)

Random forest is a decision tree-based machine learning algorithm [20]. Firstly, the bootstrap method is used to randomly draw S samples from the original training set with capacity S and repeat the operation N times to generate N sub-training sets; then for each sub-training set, the corresponding decision trees are trained and all the decision trees are integrated to form the random forest model; finally, the test set data are inputted into the random forest model and the prediction results of the random forest are generated based on all the decision trees by majority voting mechanism. The prediction results of the random forest are generated based on the prediction results of all the decision trees.

The advantage of this algorithm is that it is naturally interpretable, and the disadvantage is that it may be overfitted.

As the random forest algorithm can only perform single-factor analysis for the output, here, we only show the graphs of the importance of the influencing factors for the tree species Scotch pine. In Figure 2, it can be clearly seen that the importance of the fourth eigenvalue is significantly higher than the other input variables, which represent feeding speed, duration, temperature, and adhesives; that is, compared with the four, adhesives have the greatest influence on the surface bond strength of this species. The results for the other three species are also the same and will not be repeated here, and the results of the effects of each type of tree species will be added in the supplementary file. The results of the combined ANOVA show that both temperature and adhesives have the greatest effects on the output data.

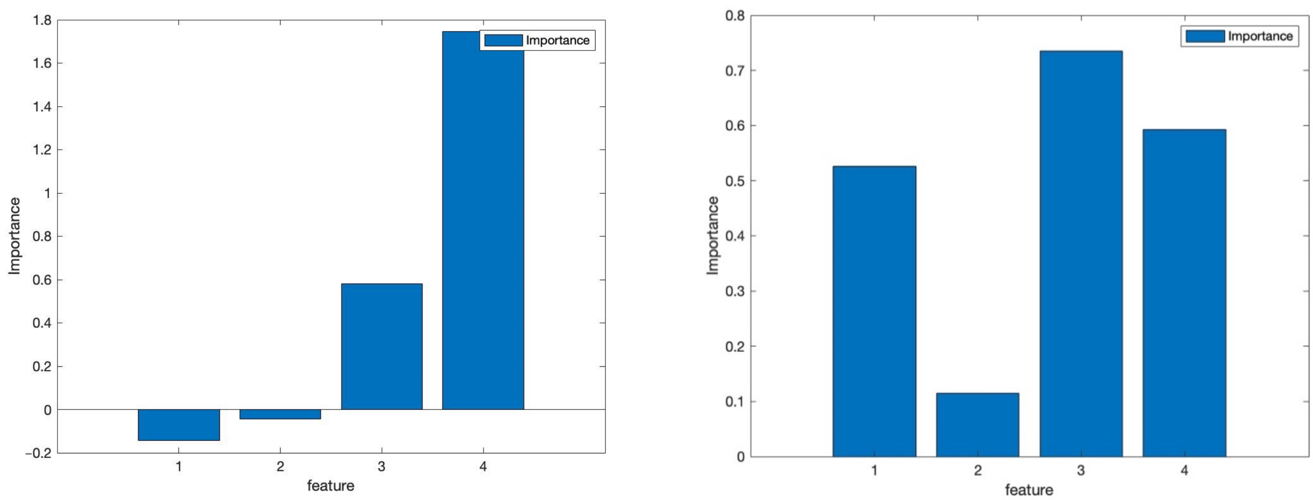

(**a**) (**b**)

Figure 2. (**a**) is the result of the analysis of decision variables for surface bond strength, and (**b**) is the result of the analysis of decision variables for surface roughness.

The random forest judgment of the decision factor can only have an approximate result, and this result is not very stable, so it needs to be combined with an SPSS *t*-test and ANOVA to further determine which independent variable causes more influence on the result. Figure 2 is only an analysis of one of the tree species, where it is only further verified that the independent variables of the outcome variables affecting the surface bond strength are the temperature and binder type, while for surface roughness, all of the variables except the second time variable have some influence on the outcome.

2.2.4. Model Performance Evaluation

Here, the mean square error (MSE), the mean absolute percentage ($MAPE$), the root mean square error ($RMSE$), and the coefficient of determination (R^2) are used to evaluate the prediction results, and the formula is expressed as:

$$MSE = \frac{1}{N}\sum_{i=1}^{N}(t_i - td_i)^2 \tag{10}$$

$$MAPE = \frac{1}{N}\left\{\sum_{i=1}^{N}\left[\left|\frac{t_i - td_i}{t_i}\right|\right]\right\} \times 100 \tag{11}$$

$$RMSE = \sqrt{\frac{1}{N}\sum_{i=1}^{N}(t_i - td_i)^2} \tag{12}$$

$$R^2 = 1 - \frac{\sum_{i=1}^{N}(t_i - td_i)^2}{\sum_{i=1}^{N}\left(\overline{td_i} - td_i\right)^2} \tag{13}$$

t_i is the measured value of the experimental sample; td_i is the predicted value; N is the total number of samples.

3. Results

Tables 5–7 show the prediction results of CPA-BP.

Table 5. The measured and the predicted values of bonding strength.

Grain Orientation	Feeding Speed	Duration	Temperature	Adhesives	Measured	Predicted	Measured	Predicted	Measured	Predicted	Measured	Predicted
					Scotch Pine		Uludag Fir		Oriental Beech		White Oak	
Radial	8 m/min	2	control	MUF	7.3000	7.6794	6.7000	6.9424	10.0000	10.5935	12.5000	11.9949
				PVAc	12.4000	12.9384	10.5000	10.4530	15.0000	15.8804	19.9000	18.7821
			120 °C	MUF	6.3000	6.4347	6.3000	6.5158	9.8000	9.9229	10.8000	10.9303
				PVAc	12.1000	12.1663	9.6000	9.7772	14.8000	15.4382	17.5000	17.5013
			150 °C	MUF	5.7000	5.9203	6.7000	6.4052	9.2000	9.0955	10.2000	9.8968
				PVAc	10.7000	10.4410	9.1000	8.8727	14.4000	14.3814	15.5000	15.7770
			180 °C	MUF	5.5000	5.6752	5.6000	5.9294	8.1000	8.2383	7.6000	8.2307
				PVAc	9.0000	9.6808	8.4000	8.5099	14.8000	13.9525	14.5000	15.5375
		4	control	MUF	7.3000	7.5344	6.7000	6.8204	9.9000	9.6859	12.5000	12.2787
				PVAc	11.7000	12.8628	10.3000	10.4035	16.1000	16.4593	16.8000	18.7292
			120 °C	MUF	7.1000	7.4255	6.3000	6.3918	9.2000	9.5855	10.1000	9.8694
				PVAc	10.2000	10.8839	9.6000	9.6280	15.4000	15.7163	15.3000	16.6434
			150 °C	MUF	5.8000	6.9837	5.5000	6.4414	8.6000	8.8279	9.0000	8.5835
				PVAc	8.1000	8.8735	8.6000	8.5327	14.7000	14.6435	14.6000	14.5109
			180 °C	MUF	5.2000	6.0050	5.1000	6.6618	8.3000	7.9627	7.3000	8.0013
				PVAc	7.8000	8.7073	8.0000	8.0996	14.1000	14.1328	14.1000	14.6037
	16 m/min	2	control	MUF	7.0000	6.6605	6.5000	7.0236	9.3000	9.3826	10.8000	10.7860
				PVAc	11.6000	12.5449	9.8000	10.1550	15.3000	16.1866	17.1000	16.8517
			120 °C	MUF	6.2000	6.2485	6.1000	6.2210	9.1000	9.2409	9.9000	9.9950
				PVAc	10.1000	10.5053	9.1000	9.0906	15.1000	15.4207	14.5000	15.5957
			150 °C	MUF	5.8000	5.5346	5.9000	5.8056	8.8000	8.5312	8.6000	8.8172
				PVAc	9.7000	9.2768	9.0000	8.5314	14.5000	14.6034	14.0000	14.8537
			180 °C	MUF	5.2000	5.1466	5.5000	5.4186	8.4000	7.8365	7.6000	7.8345
				PVAc	8.4000	8.6401	8.1000	8.1266	15.1000	14.1342	13.7000	14.2061
		4	control	MUF	7.0000	6.7588	6.2000	6.9059	9.2000	9.3938	10.8000	10.7105
				PVAc	11.6000	12.2452	9.6000	10.2657	15.3000	16.3239	17.1000	17.0773
			120 °C	MUF	6.6000	6.3451	5.9000	6.6460	8.7000	9.1959	8.8000	9.9380
				PVAc	11.3000	11.2903	9.6000	9.7277	14.9000	15.5982	15.1000	15.1886
			150 °C	MUF	6.4000	5.6998	5.3000	5.9860	8.5000	8.5284	8.3000	8.5077
				PVAc	10.2000	10.0936	8.3000	8.9364	14.8000	14.9623	14.9000	14.0068
			180 °C	MUF	5.9000	5.4324	5.0000	5.3976	8.0000	8.0672	7.2000	7.6578
				PVAc	8.9000	9.0611	8.1000	8.0123	15.0000	14.4797	14.1000	13.7108

Table 5. *Cont.*

Grain Orientation	Feeding Speed	Duration	Temperature	Adhesives	Measured	Predicted	Measured	Predicted	Measured	Predicted	Measured	Predicted
					Scotch Pine		Uludag Fir		Oriental Beech		White Oak	
Tangential	8 m/min	2	control	MUF	7.7000	7.6794	7.0000	6.9424	11.2000	10.5935	11.9000	11.9949
				PVAc	13.9000	12.9384	10.7000	10.4530	17.5000	15.8804	18.1000	18.7821
			120 °C	MUF	7.2000	6.4347	6.9000	6.5158	9.6000	9.9229	10.2000	10.9303
				PVAc	12.1000	12.1663	9.3000	9.7772	16.1000	15.4382	17.3000	17.5013
			150 °C	MUF	6.8000	5.9203	6.5000	6.4052	8.9000	9.0955	8.5000	9.8968
				PVAc	10.5000	10.4410	9.1000	8.8727	15.9000	14.3814	16.6000	15.7770
			180 °C	MUF	6.0000	5.6752	6.2000	5.9294	8.1000	8.2383	8.1000	8.2307
				PVAc	10.1000	9.6808	8.4000	8.5099	14.2000	13.9525	15.7000	15.5375
		4	control	MUF	7.7000	7.5344	7.0000	6.8204	11.2000	9.6859	11.9000	12.2787
				PVAc	13.9000	12.8628	10.7000	10.4035	17.5000	16.4593	18.7000	18.7292
			120 °C	MUF	7.5000	7.4255	6.6000	6.3918	9.8000	9.5855	9.7000	9.8694
				PVAc	11.2000	10.8839	9.6000	9.6280	16.4000	15.7163	17.7000	16.6434
			150 °C	MUF	6.9000	6.9837	6.4000	6.4414	8.7000	8.8279	8.6000	8.5835
				PVAc	10.6000	8.8735	9.1000	8.5327	14.9000	14.6435	15.1000	14.5109
			180 °C	MUF	5.9000	6.0050	6.7000	6.6618	8.0000	7.9627	8.2000	8.0013
				PVAc	9.4000	8.7073	8.2000	8.0996	14.1000	14.1328	14.9000	14.6037
	16 m/min	2	control	MUF	6.8000	6.6605	7.4000	7.0236	9.7000	9.3826	10.5000	10.7860
				PVAc	12.6000	12.5449	10.4000	10.1550	16.8000	16.1866	16.9000	16.8517
			120 °C	MUF	6.3000	6.2485	7.3000	6.2210	9.3000	9.2409	9.8000	9.9950
				PVAc	10.8000	10.5053	8.6000	9.0906	14.9000	15.4207	16.1000	15.5957
			150 °C	MUF	5.9000	5.5346	6.7000	5.8056	8.2000	8.5312	8.4000	8.8172
				PVAc	9.4000	9.2768	8.2000	8.5314	14.7000	14.6034	15.0000	14.8537
			180 °C	MUF	5.1000	5.1466	6.4000	5.4186	7.4000	7.8365	8.3000	7.8345
				PVAc	8.9000	8.6401	8.0000	8.1266	14.3000	14.1342	14.5000	14.2061
		4	control	MUF	6.8000	6.7588	7.4000	6.9059	9.7000	9.3938	10.5000	10.7105
				PVAc	12.6000	12.2452	10.7000	10.2657	16.8000	16.3239	16.9000	17.0773
			120 °C	MUF	6.0000	6.3451	7.0000	6.6460	9.6000	9.1959	10.0000	9.9380
				PVAc	10.8000	11.2903	9.9000	9.7277	16.3000	15.5982	15.6000	15.1886
			150 °C	MUF	5.4000	5.6998	6.7000	5.9860	8.1000	8.5284	8.7000	8.5077
				PVAc	10.2000	10.0936	8.9000	8.9364	15.6000	14.9623	14.6000	14.0068
			180 °C	MUF	5.0000	5.4324	5.9000	5.3976	7.1000	8.0672	8.3000	7.6578
				PVAc	9.0000	9.0611	7.7000	8.0123	14.3000	14.4797	13.1000	13.7108

Table 6. The measured and the predicted values of surface roughness (Ra).

Grain Orientation	Feeding Speed	Time	Temp.	Process	Scotch Pine		Uludag Fir		Oriental Beech		White Oak	
					Ra	Predicted Value	Ra	Predicted Value	Ra	Predicted Value	Ra	Predicted Value
Radial	8 m/min	2 h		Contr	4.320	3.993	3.670	3.765	5.980	5.563	7.440	7.239
			120 °C	b-ht	4.290	3.661	3.580	3.648	5.400	5.123	6.420	6.735
				a-ht	4.060	3.454	3.340	3.508	5.220	4.919	6.390	6.489
			150 °C	b-ht	4.130	3.515	3.320	3.497	5.170	4.909	6.200	6.413
				a-ht	3.770	3.370	3.270	3.391	5.160	4.740	6.190	6.227
			180 °C	b-ht	4.020	3.398	3.250	3.354	5.140	4.673	6.120	6.186
				a-ht	3.780	3.307	3.170	3.292	5.120	4.573	6.120	6.079
		6 h		Contr	4.370	4.363	3.640	3.707	5.870	5.821	8.160	8.028
			120 °C	b-ht	4.010	4.221	3.590	3.434	5.240	5.017	7.010	7.063
				a-ht	3.700	3.594	3.260	3.298	4.970	4.864	6.610	6.595
			150 °C	b-ht	3.970	4.009	3.570	3.329	5.310	4.716	6.890	6.614
				a-ht	3.610	3.477	3.210	3.220	4.860	4.594	6.250	6.289
			180 °C	b-ht	3.870	3.798	3.630	3.239	5.400	4.458	7.480	6.307
				a-ht	3.440	3.397	3.060	3.167	4.860	4.393	6.170	6.130
	16 m/min	2 h		Contr	4.900	4.800	3.940	4.134	6.190	5.827	8.390	8.300
			120 °C	b-ht	4.715	4.969	3.830	4.178	5.580	5.424	8.340	7.674
				a-ht	4.620	4.733	3.580	4.181	5.270	5.385	7.780	7.364
			150 °C	b-ht	5.580	4.685	3.490	3.972	4.950	5.130	7.120	7.076
				a-ht	5.420	4.275	3.430	3.915	4.620	5.083	6.320	6.697
			180 °C	b-ht	4.310	4.262	3.340	3.704	4.470	4.793	6.010	6.532
				a-ht	4.200	3.800	3.210	3.614	4.230	4.752	5.850	6.251
		6 h		Contr	4.900	4.838	4.650	4.213	5.850	5.808	9.490	8.709
			120 °C	b-ht	4.440	4.666	4.040	3.774	5.630	5.460	8.030	8.026
				a-ht	4.380	4.656	3.750	3.688	5.510	5.471	7.400	7.368
			150 °C	b-ht	4.220	4.509	3.660	3.586	5.440	5.155	7.060	7.352
				a-ht	4.160	4.255	3.550	3.456	5.400	5.208	6.340	6.637
			180 °C	b-ht	4.070	4.281	3.470	3.402	5.250	4.810	6.050	6.714
				a-ht	3.900	3.873	3.350	3.279	5.180	4.909	5.900	6.221
Tangential	8 m/min	2 h		Contr	3.600	3.993	3.910	3.765	5.060	5.563	7.000	7.239
			120 °C	b-ht	3.530	3.661	3.810	3.648	5.000	5.123	6.910	6.735
				a-ht	3.300	3.454	3.480	3.508	4.670	4.919	6.360	6.489
			150 °C	b-ht	3.280	3.515	3.380	3.497	4.590	4.909	6.230	6.413
				a-ht	3.220	3.370	3.320	3.391	4.450	4.740	6.170	6.227

Table 6. *Cont.*

Grain Orientation	Feeding Speed	Time	Temp.	Process	Scotch Pine		Uludag Fir		Oriental Beech		White Oak	
					Ra	Predicted Value	Ra	Predicted Value	Ra	Predicted Value	Ra	Predicted Value
			180 °C	b-ht	3.150	3.398	3.180	3.354	4.420	4.673	6.080	6.186
				a-ht	3.200	3.307	3.760	3.292	3.950	4.573	6.070	6.079
		6 h		Contr	4.880	4.363	3.620	3.707	5.060	5.821	6.940	8.028
			120 °C	b-ht	4.340	4.221	3.430	3.434	5.060	5.017	6.880	7.063
				a-ht	3.800	3.594	3.430	3.298	4.680	4.864	6.530	6.595
			150 °C	b-ht	3.770	4.009	3.330	3.329	4.290	4.716	6.470	6.614
				a-ht	3.760	3.477	3.120	3.220	4.160	4.594	6.300	6.289
			180 °C	b-ht	3.750	3.798	3.030	3.239	4.120	4.458	6.270	6.307
				a-ht	3.710	3.397	2.970	3.167	4.070	4.393	6.160	6.130
	16 m/min	2 h		Contr	4.860	4.800	4.850	4.134	5.480	5.827	7.780	8.300
			120 °C	b-ht	4.500	4.969	4.810	4.178	5.400	5.424	7.720	7.674
				a-ht	4.190	4.733	4.630	4.181	4.330	5.385	7.300	7.364
			150 °C	b-ht	4.090	4.685	4.520	3.972	5.330	5.130	7.060	7.076
				a-ht	3.890	4.275	4.340	3.915	5.280	5.083	6.970	6.697
			180 °C	b-ht	3.810	4.262	4.140	3.704	5.250	4.793	6.880	6.532
				a-ht	3.780	3.800	3.570	3.614	4.940	4.752	6.720	6.251
		6 h		Contr	4.880	4.838	3.850	4.213	5.480	5.808	7.760	8.709
			120 °C	b-ht	4.800	4.666	3.690	3.774	5.400	5.460	7.750	8.026
				a-ht	4.780	4.656	3.540	3.688	5.070	5.471	7.650	7.368
			150 °C	b-ht	4.680	4.509	3.450	3.586	5.270	5.155	7.440	7.352
				a-ht	4.550	4.255	3.370	3.456	4.840	5.208	7.080	6.637
			180 °C	b-ht	4.480	4.281	3.240	3.402	4.540	4.810	6.980	6.714
				a-ht	4.270	3.873	3.150	3.279	4.480	4.909	6.770	6.221

Table 7. The measured and the predicted values of surface roughness (Rmax).

Grain Orientation	Feeding Speed	Time	Temp.	Process	Scotch Pine		Uludag Fir		Oriental Beech		White Oak	
					Rmax	Predicted Value	Rmax	Predicted Value	Rmax	Predicted Value	Rmax	Predicted Value
Radial	8 m/min	2 h		Contr	26.100	26.073	23.300	23.573	36.200	36.258	49.300	49.232
			120 °C	b-ht	25.600	26.919	22.100	27.559	34.000	36.147	48.900	48.245
				a-ht	25.000	26.135	21.900	29.062	33.000	33.944	46.200	46.136
			150 °C	b-ht	24.800	25.778	21.500	29.086	32.200	33.596	45.400	46.063
				a-ht	23.800	24.925	20.900	29.747	31.000	31.947	44.700	44.069
			180 °C	b-ht	23.000	24.639	20.900	30.666	30.500	31.809	43.800	43.926
				a-ht	22.300	24.158	20.800	29.069	29.900	30.994	42.900	43.289
		6 h		Contr	28.300	32.319	23.900	29.524	38.000	39.676	49.300	49.010
			120 °C	b-ht	26.200	32.844	25.200	31.187	34.300	40.759	47.900	48.653
				a-ht	24.400	30.033	22.600	29.763	32.800	37.318	46.200	46.378
			150 °C	b-ht	26.400	30.039	23.300	28.741	35.300	38.167	48.400	47.592
				a-ht	24.100	28.912	22.400	29.346	32.600	37.111	44.700	44.168
			180 °C	b-ht	26.200	28.570	23.500	27.241	36.600	37.725	47.800	45.221
				a-ht	23.500	28.009	21.300	29.098	33.200	36.970	42.900	43.169
	16 m/min	2 h		Contr	38.800	39.121	38.800	35.434	42.700	46.643	49.300	49.214
			120 °C	b-ht	37.800	37.697	36.500	36.140	38.800	40.927	48.300	48.000
				a-ht	36.800	36.526	35.900	34.994	37.000	37.363	46.200	45.754
			150 °C	b-ht	35.500	35.719	34.500	34.247	35.000	40.381	45.400	45.872
				a-ht	34.500	35.401	33.300	33.557	33.000	39.230	44.700	43.787
			180 °C	b-ht	33.900	33.865	33.200	32.343	31.500	41.866	43.800	43.735
				a-ht	30.500	33.775	31.400	31.634	30.900	41.084	42.900	43.111
		6 h		Contr	35.800	39.207	29.800	30.771	42.800	46.784	49.300	48.601
			120 °C	b-ht	34.800	38.369	37.700	34.712	44.500	46.955	48.500	47.863
				a-ht	33.300	36.376	34.900	33.881	43.800	45.093	46.200	46.629
			150 °C	b-ht	32.900	36.771	34.200	33.121	43.500	45.472	45.400	46.336
				a-ht	31.700	34.178	33.000	32.603	41.100	43.566	44.700	44.377
			180 °C	b-ht	29.200	34.722	32.700	31.695	40.900	43.901	43.800	44.239
				a-ht	28.800	31.753	32.200	31.844	39.600	42.659	42.900	43.167
Tangential	8 m/min	2 h		Contr	29.800	26.073	36.200	23.573	39.900	36.258	49.300	49.232
			120 °C	b-ht	28.300	26.919	35.300	27.559	39.400	36.147	48.600	48.245
				a-ht	27.900	26.135	34.500	29.062	36.700	33.944	47.200	46.136
			150 °C	b-ht	26.500	25.778	33.500	29.086	36.400	33.596	46.400	46.063
				a-ht	26.500	24.925	33.300	29.747	33.100	31.947	44.700	44.069

Table 7. *Cont.*

Grain Orientation	Feeding Speed	Time	Temp.	Process	Scotch Pine		Uludag Fir		Oriental Beech		White Oak	
					Rmax	Predicted Value	Rmax	Predicted Value	Rmax	Predicted Value	Rmax	Predicted Value
			180 °C	b-ht	25.300	24.639	32.700	30.666	32.500	31.809	43.800	43.926
				a-ht	24.900	24.158	34.600	29.069	32.000	30.994	42.900	43.289
		6 h		Contr	36.700	32.319	34.600	29.524	41.900	39.676	49.300	49.010
			120 °C	b-ht	35.600	32.844	34.600	31.187	41.600	40.759	48.600	48.653
				a-ht	34.200	30.033	34.000	29.763	40.400	37.318	47.200	46.378
			150 °C	b-ht	33.400	30.039	33.600	28.741	40.100	38.167	46.400	47.592
				a-ht	32.400	28.912	32.700	29.346	39.800	37.111	44.700	44.168
			180 °C	b-ht	31.800	28.570	31.700	27.241	39.000	37.725	44.200	45.221
				a-ht	31.200	28.009	35.500	29.098	39.000	36.970	42.900	43.169
	16 m/min	2 h		Contr	39.900	39.121	35.300	35.434	47.000	46.643	49.300	49.214
			120 °C	b-ht	38.900	37.697	35.300	36.140	46.600	40.927	48.700	48.000
				a-ht	36.500	36.526	34.100	34.994	45.900	37.363	47.200	45.754
			150 °C	b-ht	35.800	35.719	33.700	34.247	44.100	40.381	46.400	45.872
				a-ht	34.600	35.401	32.500	33.557	43.600	39.230	44.700	43.787
			180 °C	b-ht	34.600	33.865	31.600	32.343	43.200	41.866	43.800	43.735
				a-ht	34.200	33.775	31.100	31.634	43.100	41.084	42.900	43.111
		6 h		Contr	42.300	39.207	33.100	30.771	49.300	46.784	49.300	48.601
			120 °C	b-ht	39.900	38.369	33.000	34.712	48.100	46.955	48.200	47.863
				a-ht	37.200	36.376	32.700	33.881	47.200	45.093	47.200	46.629
			150 °C	b-ht	36.800	36.771	32.000	33.121	46.400	45.472	46.400	46.336
				a-ht	35.300	34.178	31.100	32.603	44.700	43.566	44.700	44.377
			180 °C	b-ht	34.200	34.722	29.000	31.695	43.800	43.901	43.800	44.239
				a-ht	34.000	31.753	28.800	31.844	42.900	42.659	42.900	43.167

Table 5 is the comparison of the measured and predicted values of bond strength of different tree species under different conditions.

Tables 8–10 show the comparison results of the real measured and predicted values of the improved BP neural network by CPA, respectively. It can be seen that the prediction accuracy of the improved BP neural network is very high.

Table 8. ERROR comparison (bonding strength).

Duration	Temp.	Adhesives	Scotch Pine		Uludag Fir		Oriental Beech		White Oak	
			BP	CPA-BP	BP	CPA-BP	BP	CPA-BP	BP	CPA-BP
2	control	MUF	2.3000	−0.3794	−0.1965	−0.2424	−0.8923	−0.5935	0.7375	0.5051
		PVAc	0.8754	−0.5384	−0.1178	0.0470	−0.2607	−0.8804	0.6785	1.1179
	120 °C	MUF	1.3000	−0.1347	−0.3071	−0.2158	−0.0517	−0.1229	0.4187	−0.1303
		PVAc	−0.1163	−0.0663	0.5443	−0.1772	−0.8035	−0.6382	−0.2912	−0.0013
	150 °C	MUF	0.7000	−0.2203	0.0538	0.2948	−0.1118	0.1045	0.3549	0.3032
		PVAc	−0.8092	0.2590	0.6326	0.2273	−0.9883	0.0186	−1.6628	−0.2770
	180 °C	MUF	0.5000	−0.1752	−0.2999	−0.3294	−0.0516	−0.1383	−0.3076	−0.6307
		PVAc	−1.6752	−0.6808	0.7501	−0.1099	−0.2336	0.8475	−1.6490	−1.0375
4	control	MUF	2.2995	−0.2344	0.0459	−0.1204	−0.0679	0.2141	−0.1030	0.2213
		PVAc	3.9851	−1.1628	0.0921	−0.1035	−0.0967	−0.3593	0.0916	−1.9292
	120 °C	MUF	2.1000	−0.3255	−0.1559	−0.0918	−0.2055	−0.3855	0.2194	0.2306
		PVAc	3.0304	−0.6839	0.0095	−0.0280	−1.0313	−0.3163	−2.2387	−1.3434
	150 °C	MUF	0.8000	−1.1837	−1.0576	−0.9414	−0.6973	−0.2279	−0.3269	0.4165
		PVAc	0.7763	−0.7735	0.1211	0.0673	−1.8866	0.0565	−3.1429	0.0891
	180 °C	MUF	0.2000	−0.8050	−0.7445	−1.5618	0.2469	0.3373	−0.4554	−0.7013
		PVAc	2.7607	−0.9073	−0.3902	−0.0996	0.0527	−0.0328	0.3180	−0.5037
2	control	MUF	0.1906	0.3395	−0.5897	−0.5236	−0.1421	−0.0826	0.1834	0.0140
		PVAc	−0.4853	−0.9449	−0.2844	−0.3550	−0.7038	−0.8866	0.0844	0.2483
	120 °C	MUF	−0.0003	−0.0485	−0.7309	−0.1210	−0.0154	−0.1409	−0.0727	−0.0950
		PVAc	0.1265	−0.4053	0.0165	0.0094	0.0951	−0.3207	0.0878	−1.0957
	150 °C	MUF	−0.0288	0.2654	−0.0847	0.0944	0.1792	0.2688	−0.2917	−0.2172
		PVAc	0.4736	0.4232	0.4116	0.4686	0.0189	−0.1034	−0.2886	−0.8537
	180 °C	MUF	0.1122	0.0534	−1.0233	0.0814	1.0299	0.5635	−0.9961	−0.2345
		PVAc	1.5257	−0.2401	−0.7976	−0.0266	2.6366	0.9658	−1.8685	−0.5061
4	control	MUF	1.9269	0.2412	−0.8163	−0.7059	−0.2347	−0.1938	0.9295	0.0895
		PVAc	−0.4717	−0.6452	−0.6140	−0.6657	−0.6966	−1.0239	0.1413	0.0227
	120 °C	MUF	1.5945	0.2549	−0.0144	−0.7460	−0.0262	−0.4959	0.3935	−1.1380
		PVAc	−2.1276	0.0097	−0.0258	−0.1277	−1.7965	−0.6982	−2.3840	−0.0886
	150 °C	MUF	1.3986	0.7002	−0.5344	−0.6860	0.2033	−0.0284	0.0587	−0.2077
		PVAc	−0.0580	0.1064	−0.6371	−0.6364	−0.7999	−0.1623	0.3152	0.8932
	180 °C	MUF	0.8997	0.4676	−0.2894	−0.3976	0.4055	−0.0672	−0.4935	−0.4578
		PVAc	0.1257	−0.1611	0.2218	0.0877	0.3012	0.5203	0.5925	0.3892

Table 8. *Cont.*

Duration	Temp.	Adhesives	Scotch Pine		Uludag Fir		Oriental Beech		White Oak	
			BP	CPA-BP	BP	CPA-BP	BP	CPA-BP	BP	CPA-BP
2	control	MUF	2.7000	0.0206	0.1035	0.0576	0.3077	0.6065	0.1375	−0.0949
		PVAc	2.3754	0.9616	0.0822	0.2470	2.2393	1.6196	−1.1215	−0.6821
	120 °C	MUF	2.2000	0.7653	0.2929	0.3842	−0.2517	−0.3229	−0.1813	−0.7303
		PVAc	−0.1163	−0.0663	0.2443	−0.4772	0.4965	0.6618	−0.4912	−0.2013
	150 °C	MUF	1.8000	0.8797	−0.1462	0.0948	−0.4118	−0.1955	−1.3451	−1.3968
		PVAc	−1.0092	0.0590	0.6326	0.2273	0.5117	1.5186	−0.5628	0.8230
	180 °C	MUF	1.0000	0.3248	0.3001	0.2706	−0.0516	−0.1383	0.1924	−0.1307
		PVAc	−0.5752	0.4192	0.7501	−0.1099	−0.8336	0.2475	−0.4490	0.1625
4	control	MUF	2.6995	0.1656	0.3459	0.1796	1.2321	1.5141	−0.7030	−0.3787
		PVAc	6.1851	1.0372	0.4921	0.2965	1.3033	1.0407	1.9916	−0.0292
	120 °C	MUF	2.5000	0.0745	0.1441	0.2082	0.3945	0.2145	−0.1806	−0.1694
		PVAc	4.0304	0.3161	0.0095	−0.0280	−0.0313	0.6837	0.1613	1.0566
	150 °C	MUF	1.9000	−0.0837	−0.1576	−0.0414	−0.5973	−0.1279	−0.7269	0.0165
		PVAc	3.2763	1.7265	0.6211	0.5673	−1.6866	0.2565	−2.6429	0.5891
	180 °C	MUF	0.9000	−0.1050	0.8555	0.0382	−0.0531	0.0373	0.4446	0.1987
		PVAc	4.3607	0.6927	−0.1902	0.1004	0.0527	−0.0328	1.1180	0.2963
2	control	MUF	−0.0094	0.1395	0.3103	0.3764	0.2579	0.3174	−0.1166	−0.2860
		PVAc	0.5147	0.0551	0.3156	0.2450	0.7962	0.6134	−0.1156	0.0483
	120 °C	MUF	0.0997	0.0515	0.4691	1.0790	0.1846	0.0591	−0.1727	−0.1950
		PVAc	0.8265	0.2947	−0.4835	−0.4906	−0.1049	−0.5207	1.6878	0.5043
	150 °C	MUF	0.0712	0.3654	0.7153	0.8944	−0.4208	−0.3312	−0.4917	−0.4172
		PVAc	0.1736	0.1232	−0.3884	−0.3314	0.2189	0.0966	0.7114	0.1463
	180 °C	MUF	0.0122	−0.0466	−0.1233	0.9814	0.0299	−0.4365	−0.2961	0.4655
		PVAc	2.0257	0.2599	−0.8976	−0.1266	1.8366	0.1658	−1.0685	0.2939
4	control	MUF	1.7269	0.0412	0.3837	0.4941	0.2653	0.3062	0.6295	−0.2105
		PVAc	0.5283	0.3548	0.4860	0.4343	0.8034	0.4761	−0.0587	−0.1773
	120 °C	MUF	0.9945	−0.3451	1.0856	0.3540	0.8738	0.4041	1.5935	0.0620
		PVAc	−2.6276	−0.4903	0.2742	0.1723	−0.3965	0.7018	−1.8840	0.4114
	150 °C	MUF	0.3986	−0.2998	0.8656	0.7140	−0.1967	−0.4284	0.4587	0.1923
		PVAc	−0.0580	0.1064	−0.0371	−0.0364	0.0001	0.6377	0.0152	0.5932
	180 °C	MUF	−0.0003	−0.4324	0.6106	0.5024	−0.4945	−0.9672	0.6065	0.6422
		PVAc	0.2257	−0.0611	−0.1782	−0.3123	−0.3988	−0.1797	−0.4075	−0.6108

Table 9. ERROR comparison (surface roughness—Rmax).

Grain Orientation	Feeding Speed	Time	Temp.	Process	Scotch Pine (Rmax)		Uludag Fir (Rmax)		Oriental Beech (Rmax)		White Oak (Rmax)	
					BP	CPA-BP	BP	CPA-BP	BP	CPA-BP	BP	CPA-BP
Radial	8 m/min	2 h		Contr	−0.086	0.027	−1.639	−0.273	0.014	−0.058	0.001	0.068
			120 °C	b-ht	−1.413	−1.319	0.491	−5.459	−3.108	−2.147	0.235	0.655
				a-ht	−0.350	−1.135	0.879	−7.162	−1.393	−0.944	0.379	0.064
			150 °C	b-ht	−1.973	−0.978	−0.407	−7.586	−3.327	−1.396	−1.739	−0.663
				a-ht	−0.763	−1.125	−0.064	−8.847	−0.903	−0.947	0.010	0.631
			180 °C	b-ht	−2.650	−1.639	−1.693	−9.766	−3.312	−1.309	−1.648	−0.126
				a-ht	−1.618	−1.858	−0.131	−8.269	−0.754	−1.094	−1.014	−0.389
		6 h		Contr	−4.161	−4.019	−5.328	−5.624	−2.013	−1.676	0.160	0.290
			120 °C	b-ht	−4.843	−6.644	−4.202	−5.987	−3.587	−6.459	−0.302	−0.753
				a-ht	−1.062	−5.633	−1.719	−7.163	−0.964	−4.518	−0.184	−0.178
			150 °C	b-ht	−3.468	−3.639	−5.182	−5.441	−2.355	−2.867	1.032	0.808
				a-ht	−3.010	−4.812	−4.550	−6.946	−2.875	−4.511	0.193	0.532
			180 °C	b-ht	−2.657	−2.370	−4.367	−3.741	−1.187	−1.125	1.872	2.579
				a-ht	−4.508	−4.509	−7.325	−7.798	−3.345	−3.770	−0.498	−0.269
	16 m/min	2 h		Contr	−1.310	−0.321	3.356	3.366	12.794	−3.943	0.172	0.086
			120 °C	b-ht	0.471	0.103	0.668	0.360	8.900	−2.127	0.476	0.300
				a-ht	−0.180	0.274	0.893	0.906	7.100	−0.363	−0.103	0.446
			150 °C	b-ht	−0.081	−0.219	0.366	0.253	5.100	−5.381	−0.451	−0.472
				a-ht	0.105	−0.901	0.032	−0.257	3.100	−6.230	0.113	0.913
			180 °C	b-ht	0.447	0.035	−0.101	0.857	1.600	−10.366	−0.254	0.065
				a-ht	−1.948	−3.275	0.068	−0.234	1.000	−10.184	−0.212	−0.211
		6 h		Contr	−6.499	−3.407	−2.660	−0.971	−6.011	−3.984	0.434	0.699
			120 °C	b-ht	−7.500	−3.569	1.691	2.988	−0.851	−2.455	0.122	0.637
				a-ht	−8.999	−3.076	0.809	1.019	−0.453	−1.293	−0.117	−0.429
			150 °C	b-ht	−9.400	−3.871	0.319	1.079	−0.900	−1.972	−0.520	−0.936
				a-ht	−10.599	−2.478	0.315	0.397	−2.602	−2.466	0.193	0.323
			180 °C	b-ht	−13.100	−5.522	2.151	1.005	−1.498	−3.001	−0.075	−0.439
				a-ht	−13.499	−2.953	1.966	0.356	−1.896	−3.059	−0.277	−0.267
Tangential	8 m/min	2 h		Contr	3.614	3.727	11.261	12.627	3.714	3.642	0.001	0.068
			120 °C	b-ht	1.287	1.381	13.691	7.741	2.292	3.253	−0.065	0.355
				a-ht	2.550	1.765	13.479	5.438	2.307	2.756	1.379	1.064
			150 °C	b-ht	−0.273	0.722	11.593	4.414	0.873	2.804	−0.739	0.337
				a-ht	1.937	1.575	12.336	3.553	1.197	1.153	0.010	0.631
			180 °C	b-ht	−0.350	0.661	10.107	2.034	−1.312	0.691	−1.648	−0.126
				a-ht	0.982	0.742	13.669	5.531	1.346	1.006	−1.014	−0.389

Table 9. *Cont.*

Grain Orientation	Feeding Speed	Time	Temp.	Process	Scotch Pine (Rmax)		Uludag Fir (Rmax)		Oriental Beech (Rmax)		White Oak (Rmax)	
					BP	CPA-BP	BP	CPA-BP	BP	CPA-BP	BP	CPA-BP
		6 h		Contr	4.239	4.381	5.372	5.076	1.887	2.224	0.160	0.290
			120 °C	b-ht	4.557	2.756	5.198	3.413	3.713	0.841	0.398	−0.053
				a-ht	8.738	4.167	9.681	4.237	6.636	3.082	0.816	0.822
			150 °C	b-ht	3.532	3.361	5.118	4.859	2.445	1.933	−0.968	−1.192
				a-ht	5.290	3.488	5.750	3.354	4.325	2.689	0.193	0.532
			180 °C	b-ht	2.943	3.230	3.833	4.459	1.213	1.275	−1.728	−1.021
				a-ht	3.192	3.191	6.875	6.402	2.455	2.030	−0.498	−0.269
	16 m/min	2 h		Contr	−0.210	0.779	−0.144	−0.134	17.094	0.357	0.172	0.086
			120 °C	b-ht	1.571	1.203	−0.532	−0.840	16.700	5.673	0.876	0.700
				a-ht	−0.480	−0.026	−0.907	−0.894	16.000	8.537	0.897	1.446
			150 °C	b-ht	0.219	0.081	−0.434	−0.547	14.200	3.719	0.549	0.528
				a-ht	0.205	−0.801	−0.768	−1.057	13.700	4.370	0.113	0.913
			180 °C	b-ht	1.147	0.735	−1.701	−0.743	13.300	1.334	−0.254	0.065
				a-ht	1.752	0.425	−0.232	−0.534	13.200	2.016	−0.212	−0.211
		6 h		Contr	0.001	3.093	0.640	2.329	0.489	2.516	0.434	0.699
			120 °C	b-ht	−2.400	1.531	−3.009	−1.712	2.749	1.145	−0.178	0.337
				a-ht	−5.099	0.824	−1.391	−1.181	2.947	2.107	0.883	0.571
			150 °C	b-ht	−5.500	0.029	−1.881	−1.121	2.000	0.928	0.480	0.064
				a-ht	−6.999	1.122	−1.585	−1.503	0.998	1.134	0.193	0.323
			180 °C	b-ht	−8.100	−0.522	−1.549	−2.695	1.402	−0.101	−0.075	−0.439
				a-ht	−8.299	2.247	−1.434	−3.044	1.404	0.241	−0.277	−0.267

Table 10. Model error comparison.

Model	Object of Study		Performance Criteria					
			MAPE	MSE	RMSE	MAE	RMAE	R^2
BP	bonding strength		0.0765	1.3074	1.1434	0.7380	0.8591	0.8961
	surface roughness	Ra	0.06959	0.18118	0.42565	0.32402	0.56923	0.90375
		Rmax	0.084409	22.6945	4.7639	2.9131	1.7068	0.62626
CPA-BP	bonding strength		0.0418	0.2885	0.5371	0.3989	0.6316	0.9771
	surface roughness	Ra	0.056752	0.12429	0.35255	0.26956	0.51919	0.93397
		Rmax	0.0741	10.2645	3.2038	2.3281	1.5258	0.8310
Random Forest	bonding strength		0.0788	0.8698	0.9077	0.7370	0.8521	0.8733
	surface roughness	Ra	0.0678	0.1609	0.3955	0.3185	0.5613	0.4310
		Rmax	0.0806	11.1156	3.0732	2.6126	1.5666	0.5338

Tables 8 and 9 show the comparison of the errors of the predicted values of the BP and CPA-BP algorithms on the basis of Tables 5–7. The actual values are very close to the predicted values, and the errors are mostly below 1. It can be seen that the CPA-BP algorithm used in this paper has high accuracy in predicting the bond strength of plywood, and the errors between the predicted and the measured values are very small.

Table 10 shows the performance evaluation results of the three models, that's the BP, CPA-BP, and random forest algorithms. From Table 10, it can be seen that in terms of surface bond strength, the MAE value of the BP prediction model is 0.7380, the MSE value is 1.3074, the R^2 value is 0.8961, and the MAPE value is 0.0765. The MAE value of the random forest algorithm is 0.7370, the MSE value is 0.8698, the R^2 value is 0.8733, and the MAPE value is 0.0788. In contrast, the CPA-BP neural network algorithm yielded MSE values of 0.2885, MAE values of 0.3989, R^2 values of 0.9771, and MAPE values of 0.0418. The results indicate that the CPA-BP algorithm is sufficiently accurate and reliable in predicting the bonding performance of wood exposed to different environments, facing different processing conditions, and different types of wood. In addition, the algorithm optimized by CPA is somewhat more accurate than the conventional BP neural network algorithm.

The two parameters, Ra and Rmax, are predicted separately in terms of surface roughness; Ra represents the mean value, and Rmax represents the maximum value. the MAE values of the BP prediction model are 0.324 and 2.9131, and R^2 is 0.90375 and 0.62626. The MAE values of the random forest algorithm are 0.3185 and 2.6126, and the R^2 values are 0.4310 and 0.5338. The MAE values under the CPA-BP neural network algorithm were 0.2696 and 2.3281, and the R^2 values were 0.9340 and 0.8310. The results showed that the CPA-BP algorithm was significantly better than the traditional BP neural network and random forest algorithms in predicting the surface roughness of wood exposed to different environments, faced with different processing conditions and different types of wood, with more accurate prediction accuracy.

In Table 10, it can be clearly seen that the prediction performance of random forest is highly related to the data structure, and if there are some special data, it will seriously affect the accuracy of its prediction. The difference between the highest prediction accuracy and the lowest prediction accuracy reaches 44%, which indicates that the prediction performance of the traditional random forest algorithm is very unstable. Compared with the improved BP neural network algorithm of CPA, it can be observed at a glance which is better or worse.

From Figure 3a,b, it can be seen that the BP model is the validation set that reaches the best performance at the 37th iteration, while the CPA-BP model reaches the best performance at the 9th iteration. It can be seen that the BP model has a total of 43 iterations and the CPA improved model has 15 iterations.

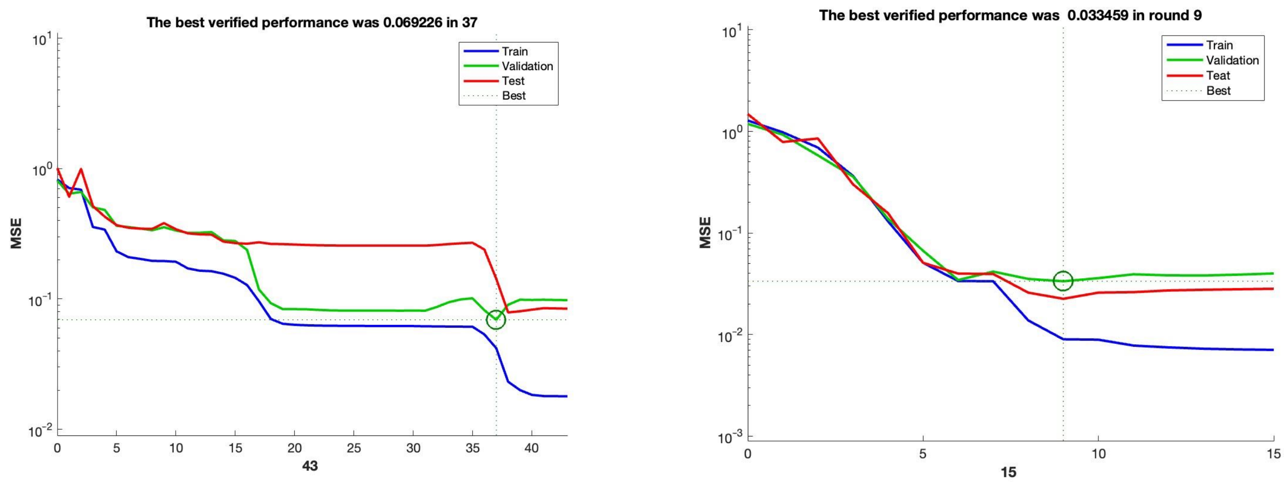

(**a**) (**b**)

Figure 3. (**a**) is the iterative curve diagram when the bond strength is predicted under the BP neural network model; (**b**) is the iterative curve diagram when the CPA-BP model is used to predict the bond strength.

From Figure 4a,b, it can be seen that in predicting the average value of surface roughness, the BP model achieves the best performance at the 15th iteration; the CPA-BP model achieves the best performance at the 7th iteration. It can be seen that the BP model has a total of 21 iterations and the CPA improved model has 13 iterations.

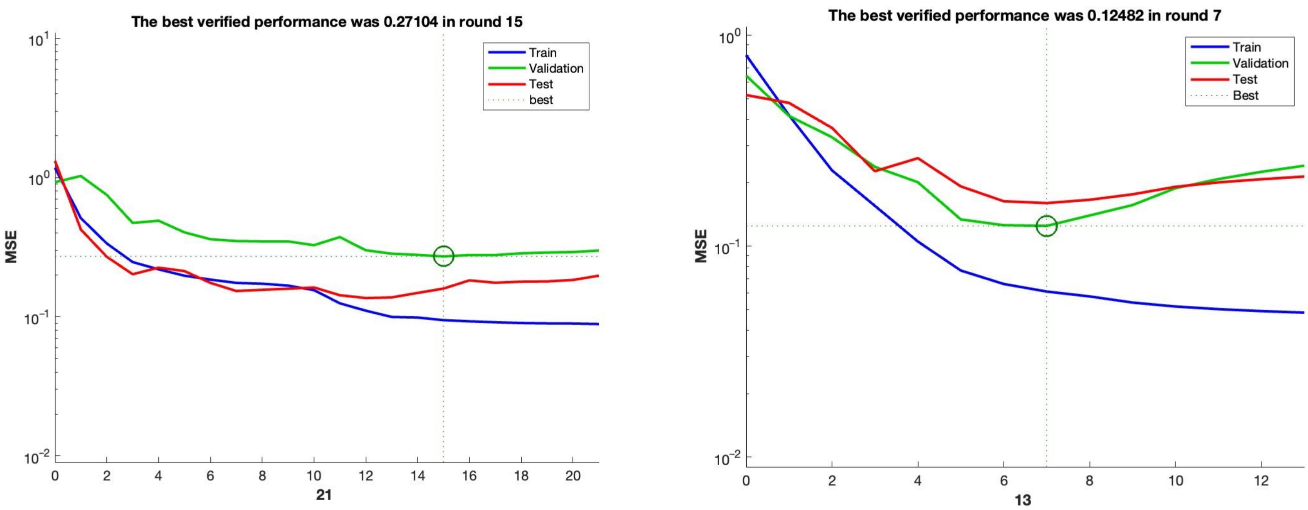

(**a**) (**b**)

Figure 4. (**a**) is an iterative graph of the prediction of surface roughness by the BP model; (**b**) is an iterative graph of the prediction of the surface roughness by the CPA-BP model.

From Figure 5a,b, it can be seen that the BP model validation set reaches the best performance at the 11th iteration, while the CPA-BP model reaches the best performance at the 3rd iteration. It can be seen that the BP model has a total of 17 iterations and the CPA improved model has 9 iterations, which shows that CPA-BP has a faster convergence rate and can save iteration time.

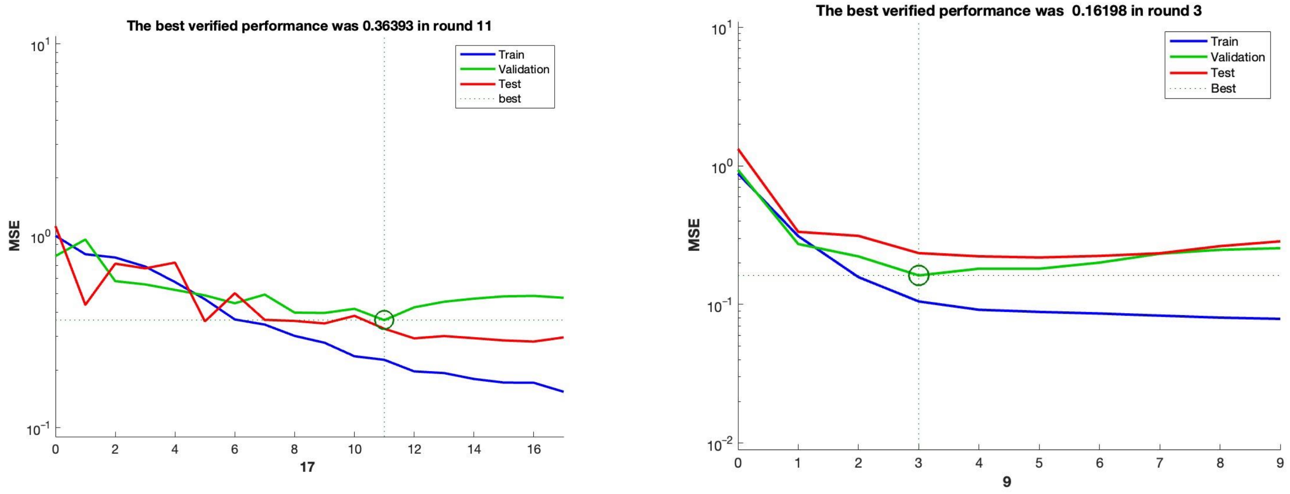

(**a**) (**b**)

Figure 5. (**a**) is an iterative graph of the prediction of the Rmax of the surface roughness by the BP model; (**b**) is an iterative graph of the prediction of the Rmax of the surface roughness by the CPA-BP model.

Figures 6–8 show that the fitting results of CPA-BP are significantly better than those of BP. The best prediction results are obtained for bonding strength, but the greatest improvement in prediction accuracy is obtained for Rmax in surface roughness.

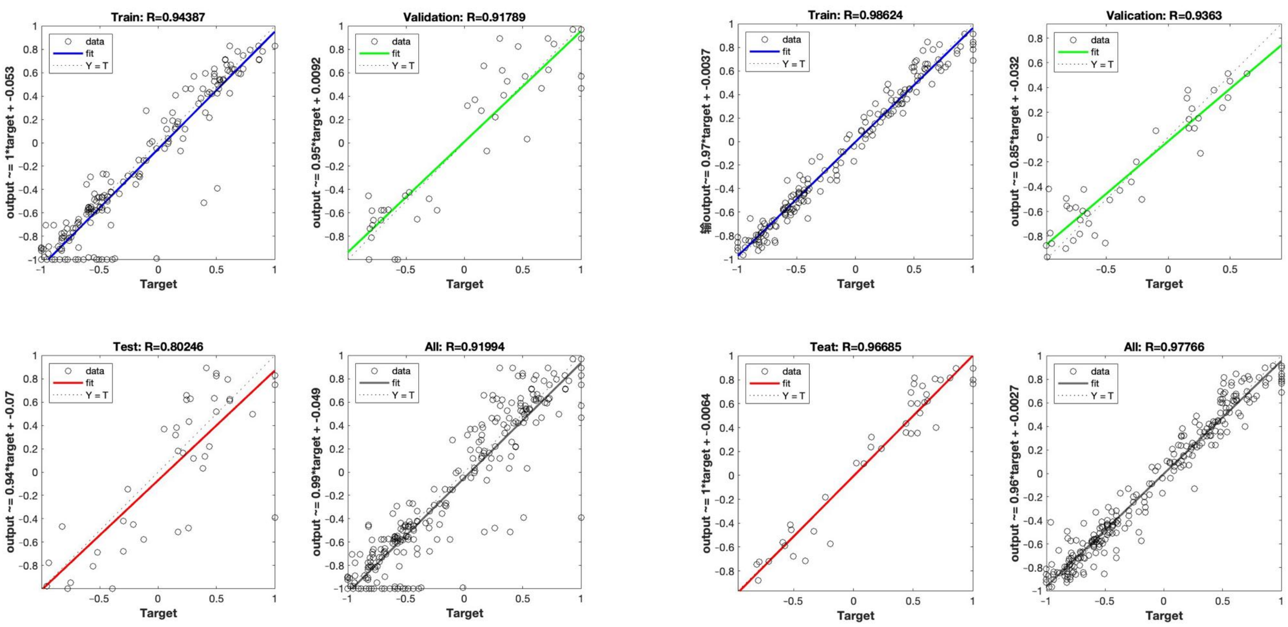

(**a**) (**b**)

Figure 6. (**a**,**b**) are two graphs showing the relationship between the training set, the validation set, and the test set predicted value and the actual value when the BP and CPA-BP model predicts the bond strength of plywood.

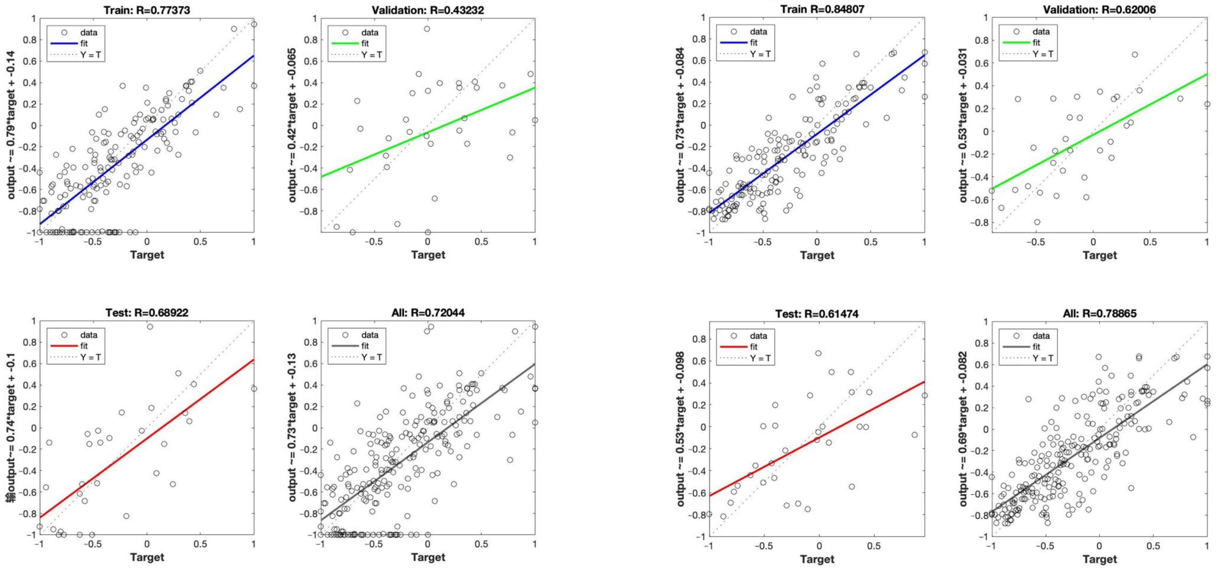

(**a**) (**b**)

Figure 7. (**a**,**b**) are two graphs showing the relationship between the training set, the validation set, and the test set predicted value and the actual value when the BP and CPA-BP model predicts the surface roughness (Ra) of plywood.

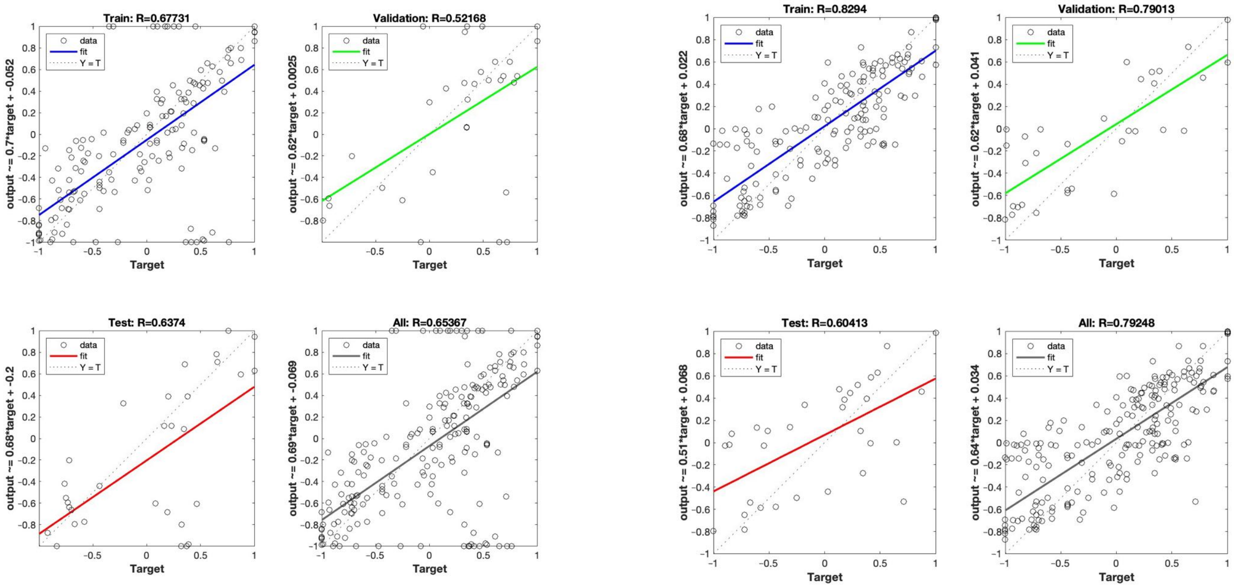

(**a**) (**b**)

Figure 8. (**a**,**b**) are two graphs showing the relationship between the training set, the validation set, and the test set predicted value and the actual value when the BP and CPA-BP model predicts the surface roughness (Rmax) of plywood.

The coefficient of determination R^2 between the measured and predicted values is an important indicator to test the validity of a predictive model. It generally ranges from 0 to 1. The closer the R^2 is to 1, the higher the prediction accuracy of the model. In general, the best measure of linear regression is R^2. As can be seen from the figure, the R^2 of the model is 8.1% greater than BP on the test set, training set, and validation set when predicting surface bond strength using the CPA-BP algorithm, while the prediction of surface roughness is increased by a maximum of 20.4% in prediction accuracy. In this paper, the R^2 values obtained using the CPA-BP algorithm are all very close to 1, indicating superiority over the conventional BP neural network model.

The blue line is the actual measured value, and the red line is the predicted value. Figures 9 and 10 show the comparison results between the predicted and actual measured values of bond strength by CPA-BP and BP, respectively, and it can be clearly seen that the prediction accuracy of CPA-BP is significantly better than that of BP.

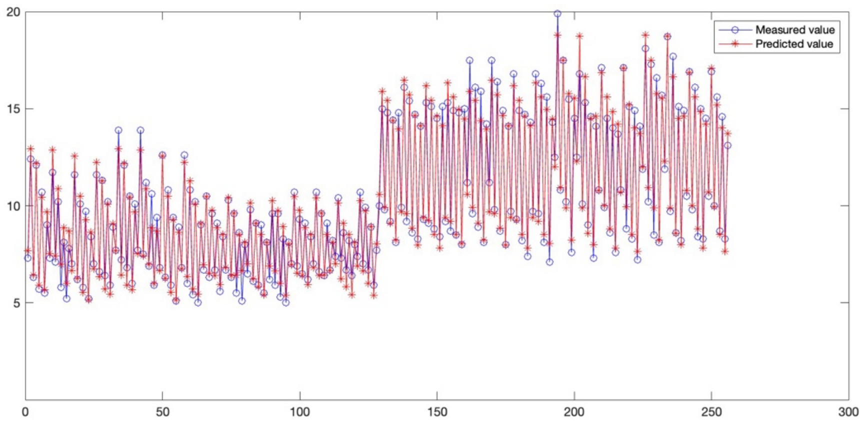

Figure 9. The comparison between the actual value of the bond strength of the plywood and the predicted value of the CPA-BP model is shown in Figure 9.

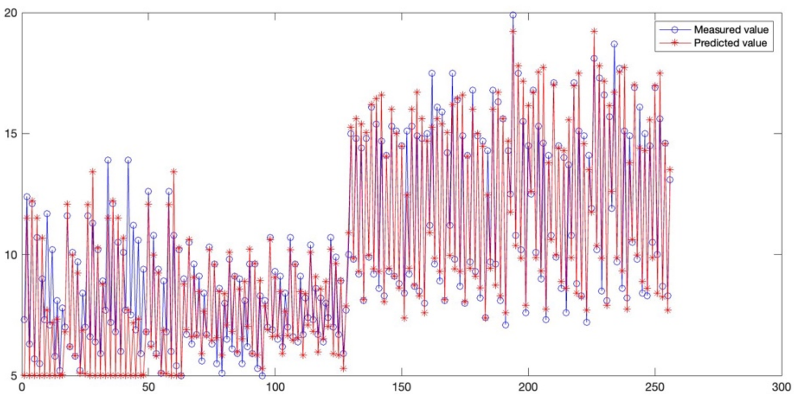

Figure 10. The comparison between the actual value of the bond strength of the plywood and the predicted value of the BP model is shown in Figure 10.

As can be seen from Figure 11, the error curve of the prediction results of CPA-BP is much flatter than that of the BP model. The smaller error proves the usability of the CPA-BP model in predicting the bond strength and also shows that the model can be used to predict the bond strength of plywood.

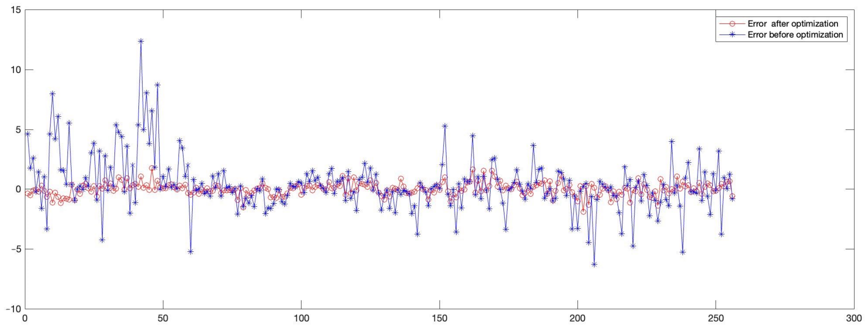

Figure 11. It is a comparison diagram of the prediction error of the BP neural network model and the CPA-BP model for the bonding strength of the plywood.

Figures 12 and 13 clearly show that the prediction accuracy of CPA-BP is significantly better than BP, and the prediction results of BP neural network in both sets of data have a large error.

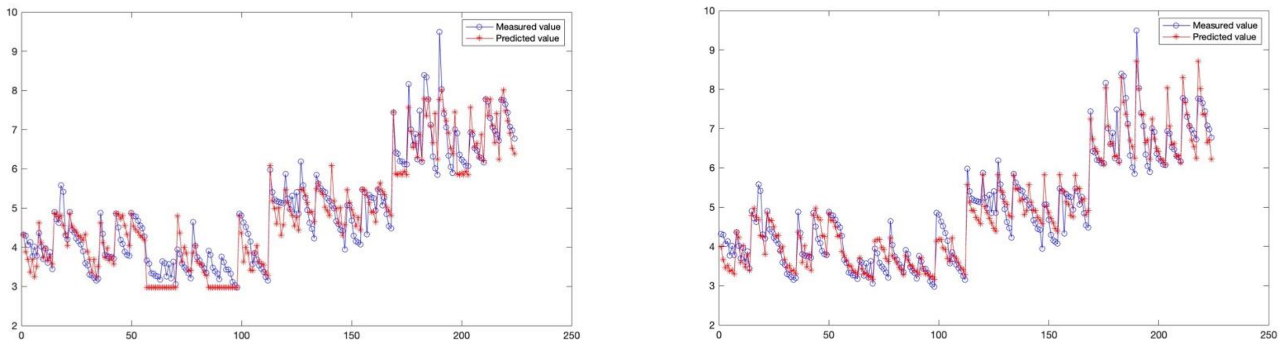

(**a**) (**b**)

Figure 12. The comparison between the actual value of the surface roughness (Ra) and the predicted value of the BP (**a**) and the CPA-BP (**b**) model is shown in Figure 12.

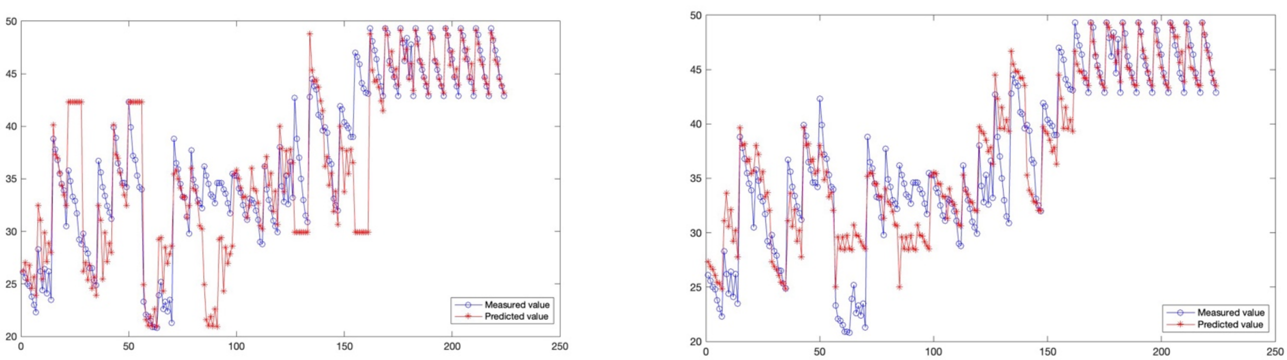

(**a**) (**b**)

Figure 13. The comparison between the actual value of the surface roughness (Rmax) and the predicted value of the BP (**a**) and the CPA-BP (**b**) model is shown in Figure 13.

As can be seen in Figure 14, the error curve of CPA-BP for the prediction of surface roughness is much flatter than that of the BP model. The smaller error proves that the CPA-BP model has a great optimization effect. It can also further prove that the prediction accuracy of CPA-BP is more accurate.

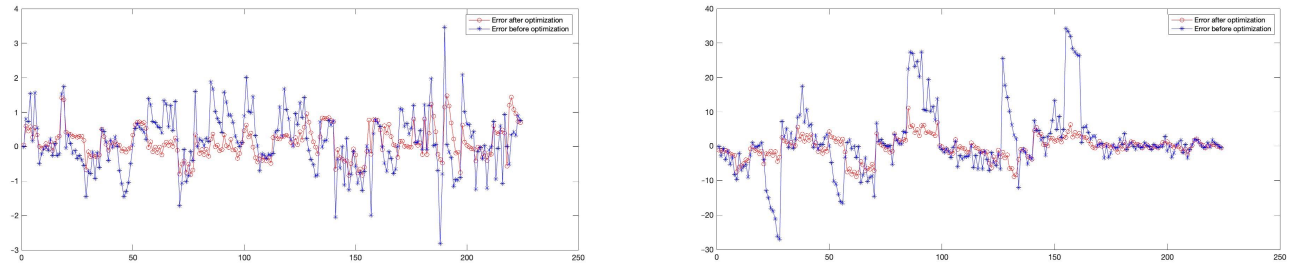

(**a**) (**b**)

Figure 14. The comparison diagram of the prediction error of the BP neural network model and the CPA-BP model for the surface roughness (Ra (**a**) and Rmax (**b**)) of plywood.

Since the traditional random forest algorithm can only have one predicted output value, the prediction result of the scotch pine tree species is selected here as a representative for analysis (the prediction results of other tree species are shown in the Supplementary File).

From Figures 15 and 16, it can be observed intuitively that the random forest prediction results are not very satisfactory, especially in the part of the test set where the error is large, and in connection with Table 10 mentioned above, it can be found that the performance of the model is unsatisfactory.

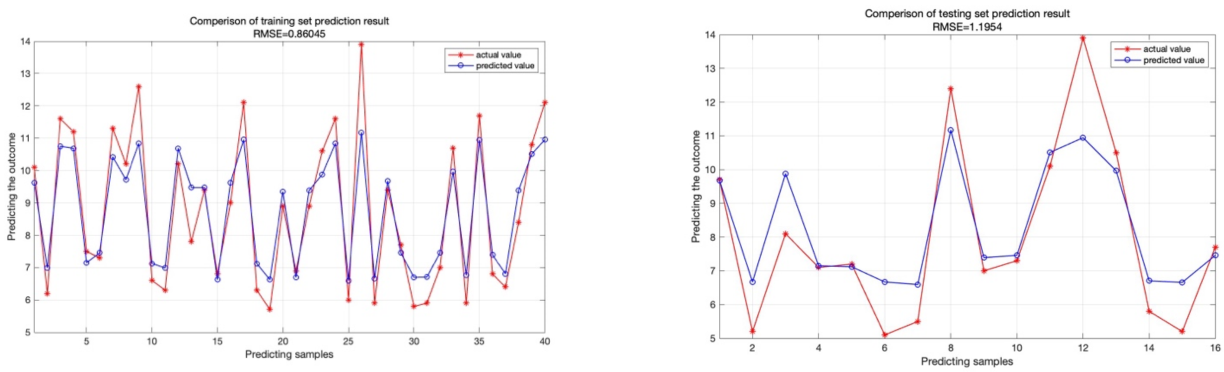

(**a**) (**b**)

Figure 15. It is the comparative results of surface bonding strength prediction using the random forest algorithm when the tree species is Scotch pine, (**a**) for the training set and (**b**) for the test set.

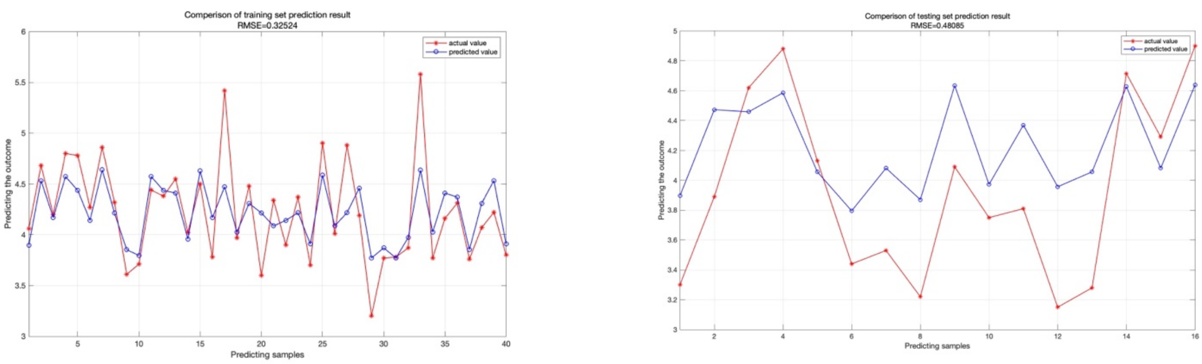

(**a**) (**b**)

Figure 16. It is the comparative results of surface roughness prediction using the random forest algorithm when the tree species is Scotch pine (Ra), (**a**) for the training set and (**b**) for the test set.

4. Discussion

- The four variables of feed rate, wood species, heat treatment time, and heat treatment temperature were varied to varying degrees in this paper. The bond strength values of the two adhesives, PVAc and MUF, were predicted according to varying degrees of changes in different variables. It can be seen from Table 1 that with the increase in temperature, the bonding strength of the PVAc and MUF adhesives gradually decreases, and the value of the PVAc bonding strength decreases significantly between different tree species. Therefore, the CPA-BP model can be used as an efficient method to predict the optimal bond strength of different wood species processed and heat treated under different conditions. Miao SU et al. [21] used an artificial neural network to predict surface-embedded fibers to enhance the bond strength between CFRP and concrete. The established BPNN model has a coefficient of determination R^2 of 0.957. Julian D Olden et al. [22] used a Monte Carlo simulation to provide a comparison of the results of different methods. Their paper showed that the average similarity between the actual and predicted values obtained using this method was 0.92; Mário R.F. Coelho et al. [23] proposed a DM model to predict the NSM FRP system, the bond strength of which is more robust and accurate than the guide model, with a minimum RMSE value of 8.6 and an R^2 of 0.89. However, the CPA-BP algorithm used in this paper has a better performance in the relationship between the actual value and the predicted value. The coefficient of determination is 0.9771.
- The tree species of the wood is also an important factor affecting the glue strength. Studies have shown that when the wood is glued with the same kind of adhesive, the glue strength also increases proportionally with the density of the tree species. White oak has the greatest bond strength of the four tree species mentioned in this article. On the influence of the direction of wood grain, changing the direction of the fibers on the surface of the plywood, the glued strength will also change accordingly. The bonding strength of the two pieces of wood fiber is the highest when the direction of the wood fibers is parallel, and the bonding strength is the lowest when the direction of the two wood fibers is perpendicular. Ayhan Özçifçi et al. (2008) [24] mentioned in their paper that beech wood has a high density, and its bond strength is better in the tangential direction than in the radial direction. Among all the factors that affect the bonding strength of wood, the relationship between the surface roughness and the bonding strength is relatively complex, and parameters such as wood properties and processing methods may affect the surface roughness, thereby affecting the bonding effect. The bonding strength of the wood surface does not increase linearly with the decrease in the surface roughness. The heat treatment of wood improves its elasticity and mechanical properties, and it is a common process today to maintain the quality of wood by changing its equilibrium moisture content, surface bond strength, surface roughness, etc. In summary, predicting wood properties is relevant to improving wood utilization [25].

5. Conclusions

- In this paper, a CPA-BP model was used to predict the bond strength and surface roughness of four kinds of wood with feeding speed, heat treatment time, temperature, and adhesive type as input variables, and they were compared with the actual measured values. The two prediction models used 64 and 56 sets of data, respectively, and were divided into two training and test sets for predicting the bond strength and surface roughness, respectively. The results showed that the optimized bond strength prediction results using the CPA-BP model resulted in a 77.9% decrease in MSE value, a 45.9% decrease in MAE value, a 45.35% decrease in MAPE value, and a 9% increase in R^2 value compared to the BP neural network, as well as an 11.9% increase in R^2 compared to the random forest algorithm. The surface roughness prediction results showed that the optimized MSE values decreased by up to 54.77%, MAE values decreased by 20.8%, MAPE values decreased by 12.2%, and R^2 values increased by 39.4%;

compared with the random forest algorithm, R^2 increased by up to 55.6%. It can be seen that the algorithm used in this paper has higher accuracy compared to the BP algorithm.

- Combining with the data set used in this paper, there are four types of input, and there is a complex linear relationship between the input and the output. The BP neural network model optimized by CPA has also achieved ideal results in prediction. According to the comparison between the predicted value and the measured value, when the R^2 between them is very close to 1, the various error values and MAPE, that is, the average error percentage, are very low. These values illustrate the accuracy and applicability of the CPA-BP algorithm. Compared with the traditional BP neural network model, the algorithm used in this paper is closer to the actual measured value.
- When heat-treating wood, the bond strength values were higher with the PVAc binder under the same tree species and white oak with the same binder. When other conditions are the same, the adhesion performance will gradually decrease with the increase in temperature, among which, the decrease in PVAc is more obvious than that of MUF. When the other conditions are the same, its bond strength is better in the tangential direction than in the radial direction. However, the relationship between surface roughness and wood glue strength is relatively complex.
- In future research, this model can be further optimized. It can be seen that although the CPA-BP model is better than the BP neural network model in predicting the glue strength and surface roughness of plywood, its effect can be better, especially on the surface. In the roughness part, the coefficient of determination R^2 of the model is 0.83, and the weights and thresholds in the algorithm can be optimized again so that the prediction results can be closer to the real value and the R^2 is higher.

Supplementary Materials: The following supporting information can be downloaded at: https://www.mdpi.com/article/10.3390/f14010051/s1, The Supplementary File.

Author Contributions: Conceptualization, Y.W.; methodology, Y.W.; software, Y.W.; validation, Y.W. and Y.C.; formal analysis, Y.W.; investigation, Y.W.; resources, Y.W.; data curation, Y.C.; writing—original draft preparation, Y.W. and Y.C.; writing—review and editing, Y.W. and Y.C.; visualization, Y.W.; supervision, W.W.; project administration, Y.W.; funding acquisition, W.W. All authors have read and agreed to the published version of the manuscript.

Funding: This research was fund by the Fundamental Research Funds for the Central Universities, grant number 2572019BL04, and the Scientific Research Foundation for the Returned Overseas Chinese Scholars of Heilongjiang Province, grant number LC201407.

Institutional Review Board Statement: Not applicable.

Informed Consent Statement: Not applicable.

Data Availability Statement: In this paper, the data are openly available in a public repository that issues datasets with DOIs. The data that support the findings of this study are openly available in Construction and Building Materials at https://doi.org/10.1016/j.conbuildmat.2012.01.008, reference number [10] (accessed on 18 November 2022).

Conflicts of Interest: The authors declare no conflict of interest.

References

1. Cai, J.; Cai, L. Effects of thermal modification on mechanical and swelling properties and color change of lumber killed by mountain pine beetle. *Bioresources* **2012**, *7*, 3488–3499. [CrossRef]
2. Schmidt, M.; Glos, P.; Wegener, G. Gluing of European beech wood for load bearing timber structures. *Eur. J. Wood Wood Prod.* **2010**, *68*, 43–57. [CrossRef]
3. Knorz, M.; Schmidt, M.; Torno, S.; Van De Kuilen, J.-W. Structural bonding of ash (Fraxinus excelsior L.): Resistance to delamination and performance in shearing tests. *Holz als Roh-und Werkst.* **2014**, *72*, 297–309. [CrossRef]
4. Sikora, K.S.; McPolin, D.O.; Harte, A.M. Shear Strength and Durability Testing of Adhesive Bonds in Cross-laminated Timber. *J. Adhes.* **2015**, *92*, 758–777. [CrossRef]

5. Hill, C.; Altgen, M.; Rautkari, L. Thermal modification of wood—A review: Chemical changes and hygroscopicity. *J. Mater. Sci.* **2021**, *56*, 6581–6614. [CrossRef]
6. Kubovský, I.; Kačíková, D.; Kačík, F. Structural Changes of Oak Wood Main Components Caused by Thermal Modification. *Polymers* **2020**, *12*, 485. [CrossRef]
7. Herrera-Builes, J.; Sepúlveda-Villarroel, V.; Osorio, J.; Salvo-Sepúlveda, L.; Ananías, R. Effect of Thermal Modification Treatment on Some Physical and Mechanical Properties of *Pinus oocarpa* Wood. *Forests* **2021**, *12*, 249. [CrossRef]
8. Wentzel, M.; Fleckenstein, M.; Hofmann, T.; Militz, H. Relation of chemical and mechanical properties of Eucalyptus nitens wood thermally modified in open and closed systems. *Wood Mater. Sci. Eng.* **2019**, *14*, 165–173. [CrossRef]
9. Wang, X.; Chen, X.; Xie, X.; Wu, Y.; Zhao, L.; Li, Y.; Wang, S. Effects of thermal modification on the physical, chemical and micromechanical properties of Masson pine wood (*Pinus massoniana* Lamb.). *Holzforschung* **2018**, *72*, 1063–1070. [CrossRef]
10. Čabalová, I.; Výbohová, E.; Igaz, R.; Kristak, L.; Kačík, F.; Antov, P.; Papadopoulos, A.N. Effect of oxidizing thermal modification on the chemical properties and thermal conductivity of Norway spruce (*Picea abies* L.) wood. *Wood Mater. Sci. Eng.* **2022**, *17*, 366–375. [CrossRef]
11. Serrano, E. A numerical study of the shear-strength-predicting capabilities of test specimens for wood–adhesive bonds. *Int. J. Adhes. Adhes.* **2004**, *24*, 23–35. [CrossRef]
12. Esteban, L.G.; Fernández, F.G.; de Palacios, P. Prediction of plywood bonding quality using an artificial neural network. *Holzforschung* **2011**, *65*, 209–214. [CrossRef]
13. Demirkir, C.; Özsahin, Ş.; Aydin, I.; Colakoglu, G. Optimization of some panel manufacturing parameters for the best bonding strength of plywood. *Int. J. Adhes. Adhes.* **2013**, *46*, 14–20. [CrossRef]
14. Ugulino, B.; Hernández, R.E. Assessment of surface properties and solvent-borne coating performance of red oak wood produced by peripheral planing. *Eur. J. Wood Wood Prod.* **2017**, *75*, 581–593. [CrossRef]
15. Hazir, E.; Ozcan, T.; Koç, K.H. Prediction of Adhesion Strength Using Extreme Learning Machine and Support Vector Regression Optimized with Genetic Algorithm. *Arab. J. Sci. Eng.* **2020**, *45*, 6985–7004. [CrossRef]
16. Ozcan, S.; Ozcifci, A.; Hiziroglu, S.; Toker, H. Effects of heat treatment and surface roughness on bonding strength. *Constr. Build. Mater.* **2012**, *33*, 7–13. [CrossRef]
17. Ong, K.M.; Ong, P.; Sia, C.K. A carnivorous plant algorithm for solving global optimization problems. *Appl. Soft Comput.* **2020**, *98*, 106833. [CrossRef]
18. Tiryaki, S.; Özşahin, Ş.; Yıldırım, I. Comparison of artificial neural network and multiple linear regression models to predict optimum bonding strength of heat treated woods. *Int. J. Adhes. Adhes.* **2014**, *55*, 29–36. [CrossRef]
19. Kohonen, T.; Mäkisara, K.; Simula, O.; Kangas, J. (Eds.) *Artificial Neural Networks*; Elsevier: Amsterdam, The Netherlands, 1991. [CrossRef]
20. Cutler, D.R.; Edwards, T.C., Jr.; Beard, K.H.; Cutler, A.; Hess, K.T.; Gibson, J.; Lawler, J.J. Random forests for classification in ecology. *Ecology* **2007**, *88*, 2783–2792. [CrossRef]
21. Su, M.; Peng, H.; Li, S.-F. Application of an interpretable artificial neural network to predict the interface strength of a near-surface mounted fiber-reinforced polymer to concrete joint. *J. Zhejiang Univ. A* **2021**, *22*, 427–440. [CrossRef]
22. Olden, J.D.; Joy, M.K.; Death, R.G. An accurate comparison of methods for quantifying variable importance in artificial neural networks using simulated data. *Ecol. Model.* **2004**, *178*, 389–397. [CrossRef]
23. Coelho, M.R.; Sena-Cruz, J.M.; Neves, L.A.; Pereira, M.; Cortez, P.; Miranda, T. Using data mining algorithms to predict the bond strength of NSM FRP systems in concrete. *Constr. Build. Mater.* **2016**, *126*, 484–495. [CrossRef]
24. Özçifçi, A.; Yapici, F. Effects of machining method and grain orientation on the bonding strength of some wood species. *J. Mater. Process. Technol.* **2008**, *202*, 353–358. [CrossRef]
25. Chen, Y.; Wang, W.; Li, N. Prediction of the equilibrium moisture content and specific gravity of thermally modified wood via an Aquila optimization algorithm back-propagation neural network model. *BioResources* **2022**, *17*, 4816–4836. [CrossRef]